

# Facile Synthesis of Gold Wavy Nanowires and Investigation of Their Growth Mechanism

Cun Zhu,<sup>†,‡</sup> Hsin-Chieh Peng,<sup>‡</sup> Jie Zeng,<sup>||</sup> Jingyue Liu,<sup>§</sup> Zhongze Gu,<sup>‡</sup> and Younan Xia<sup>\*,†,‡</sup>

<sup>†</sup>The Wallace H. Coulter Department of Biomedical Engineering, Georgia Institute of Technology and Emory University, Atlanta, Georgia 30332, United States

<sup>‡</sup>State Key Laboratory of Bioelectronics, School of Chemistry and Chemical Engineering, Southeast University, Nanjing 210096, P. R. China

<sup>‡</sup>School of Chemistry and Biochemistry, School of Chemical and Biomolecular Engineering, Georgia Institute of Technology, Atlanta, Georgia 30332, United States

<sup>||</sup>Hefei National Laboratory for Physical Sciences at the Microscale and Department of Chemical Physics, University of Science and Technology of China, Hefei, Anhui 230026, P. R. China

<sup>§</sup>Department of Physics, Arizona State University, Tempe, Arizona 85287, United States

## Supporting Information

**ABSTRACT:** We describe a synthesis of Au wavy nanowires in an aqueous solution in the presence of cetyltrimethylammonium bromide (CTAB). The resultant Au nanowires automatically separated from the solution and floated at the air/water interface. We investigated the formation mechanism by characterizing the samples obtained at different stages of the synthesis. Both particle attachment and cold welding were found to be involved in the formation of such nanowires. Based on X-ray photoelectron spectroscopy and thermogravimetric analysis, the CTAB molecules adsorbed on the surface of a Au nanostructure went through a change in structure from a bilayer to a monolayer, converting the Au surface from hydrophilic to hydrophobic. As a result, the Au wavy nanowires were driven to the air/water interface during the synthesis. This growth mechanism is potentially extendable to many other systems involving small surfactant molecules.

One-dimensional (1D) metal nanostructures in the form of wires, rods, and tubes have received great interest in recent years owing to their unique properties related to the transport of electrons, photons, and surface plasmons.<sup>1</sup> In particular, the chemical stability of Au has made its nanowires attractive building blocks for the fabrication of nanoscale photonic, electronic, and sensing devices; notable examples include plasmonic antennae, transparent electrodes, and biosensors.<sup>2</sup> As such, considerable efforts have been devoted to the synthesis of Au nanowires, and the reported protocols are typically based upon physical deposition on a patterned substrate,<sup>3</sup> assembly of particles,<sup>4</sup> seed-<sup>5</sup> and surfactant-mediated growth,<sup>6</sup> and template-assisted synthesis.<sup>7</sup>

One of the most successful protocols involves the formation of Au nanowires (and nanorods) in the presence of small surfactant molecules, such as cetyltrimethylammonium bromide (CTAB), oleic acid, or oleylamine.<sup>8</sup> These amphiphilic molecules play a central role in the synthesis by serving as a capping agent for the

surface and as soft templates to confine and direct the growth or attachment of Au atoms or nanoparticles to form nanowires. Here, the dispersion of the Au nanowires in a solution strongly depends on the surface property, which can be controlled by manipulating the assembly of the amphiphilic molecules on their surfaces. Most of the reported syntheses involved the formation of Au nanowires in the bulk of an aqueous solution, where the surfactant molecules adsorbed onto the Au surface to form a hydrophilic bilayer. There are only a few reports on the synthesis of Au nanowires with hydrophobic surfaces in an aqueous solution so the nanowires would be naturally enriched at the air/water interface. Gao et al. reported the growth of Au nanowires at the interface of air and an aqueous solution by employing a Au-coated Pt tip to initiate the growth.<sup>8f</sup> Despite their success with respect to the growth of Au nanowires with well-defined morphology at the air/water interface, they did not discuss why the Au nanowires were formed at the air/water interface. Moreover, the growth was initiated with a micrometer-sized template, which will become unfavorable for the production of Au nanowires on a large scale.

Herein, we present a facile method for generating Au wavy nanowires at room temperature. The synthesis involved the reduction of HAuCl<sub>4</sub> by ascorbic acid (AA) in the presence of CTAB, an amphiphilic molecule that could serve as both a coordination ligand for the Au ions and a capping agent for the resultant Au nanostructures. The nanowires were formed as a result of particle attachment of the initially formed Au nanoparticles, followed by cold welding, surface diffusion, and additional growth. To our surprise, the Au wavy nanowires were concentrated at the air/water interface during a synthesis. By analyzing the surface properties of the resultant Au nanostructures, we discovered that the CTAB molecules adsorbed on the surfaces of Au nanostructures went through a structural change from a hydrophilic bilayer to a hydrophobic monolayer, driving the Au wavy nanowires to the air/water interface.

Received: September 13, 2012

Published: December 4, 2012



Different from the conventional seed-mediated growth of Au nanorods with controlled aspect ratios, the Au wavy nanowires were synthesized using a one-step procedure, during which the precursor underwent a much slower reduction. In a typical synthesis, an aqueous AA solution was injected into an aqueous solution of  $\text{HAuCl}_4$  and CTAB with a pipet, followed by adding an aqueous NaOH solution (details in Supporting Information, SI). The introduction of AA immediately turned the solution from orange to colorless due to the reduction of  $\text{Au}^{\text{III}}$  to  $\text{Au}^{\text{I}}$ , thereby generating a new precursor at the +1 oxidation state.<sup>9</sup> This intermediate solution containing the  $\text{Au}^{\text{I}}$  complex could be stored at room temperature for a few hours. When aqueous NaOH at a relatively low concentration was introduced, the reducing power of AA would be enhanced to accelerate the reduction of the  $\text{Au}^{\text{I}}$  precursor.<sup>10</sup> The reaction was allowed to proceed at room temperature without disturbance for 24 h and brown materials were observed to gradually appear at the air/solution interface. Figure 1 shows a digital photograph of the reaction solution at  $t = 24$  h and electron microscopy images of the products. It can be seen that the resultant Au nanostructures mainly floated at the air/water interface whereas the bulk of the solution was transparent and essentially colorless (Figure 1A). The SEM and TEM images in Figure 1B clearly show a wire-like morphology for the products, which were mainly composed of wavy nanowires with aspect ratios larger than  $10^3$  (Figure S1 shows the aspect ratios of the resultant Au nanowires could also be varied by altering the experimental conditions). The average diameter of the wavy nanowires was 15 nm, while their lengths were up to  $100 \mu\text{m}$ . These nanowires tended to further assemble into bundles at the air/water interface. By resolving their atomic structures with high-resolution TEM (Figure 1C,D), multiple crystal domains and twin boundaries could be observed in the wavy nanowires, including both the kink and straight regions (Figures 1D and S2). In a sense, the wavy nanowire should be considered a polycrystalline rather than a single-crystal structure.

To decipher the mechanism responsible for the formation of such wavy nanowires, we collected samples at different time points for TEM characterization. Figure 2 shows a set of representative images to summarize our observations. In the initial stage of the synthesis, only spherical particles with diameters in the sub-10 nm regime were found in the solution

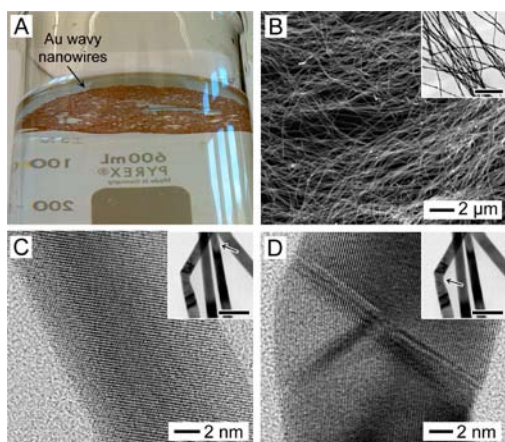


**Figure 1.** (A) Au wavy nanowires floating at the air/aqueous solution interface. (B) SEM image of the Au wavy nanowires and their corresponding TEM image (inset; scale bar is 500 nm). (C,D) High-resolution TEM images from different regions of the nanowires as marked by arrows in the insets; scale bars are 50 nm.

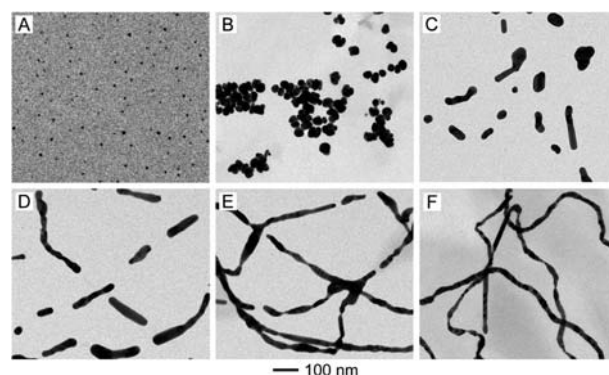


**Figure 2.** TEM images of Au nanostructures obtained after the reaction had proceeded for (A) 5, (B) 15, (C) 25, (D) 35, (E) 55, and (F) 90 min, respectively. Samples in (A–C) were obtained from the solution, whereas those in (D–F) were collected from the air/water interface.

(Figure 2A), indicating the reduction of the  $\text{Au}^{\text{I}}$  precursor into  $\text{Au}^0$  and subsequent formation of nanoparticles. After the reaction had proceeded for 15 min, larger nanoparticles with sizes on the scale of 35 nm were found in the solution (Figure 2B), which were likely formed through continuous growth of the small nanoparticles and their aggregation in an effort to reduce the surface energy. The large nanoparticles then evolved into short rods and necklace-like nanostructures when the reaction time was prolonged to 25 and 35 min (Figure 2C,D), respectively. Interestingly, the nanorods were aligned more or less along the long axis of a nanowire (Figure 2D), suggesting the possible involvement of a templating effect provided by the CTAB molecules (Figure S3). These intermediate nanostructures further grew in length (Figure 2E), and brown, cotton-like materials obviously appear at the air/water interface after the reaction had proceeded for 55 min, indicating the formation of Au wavy nanowires. When the reaction time reached 90 min, wavy nanowires with high aspect ratios were obtained (Figure 2F). At this point, a large number of convex/concave regions and kinks could still be seen on the Au nanowires. Driven by the difference in chemical potential between the convex and the concave regions,<sup>8c</sup> the Au atoms could diffuse along individual nanowires to generate smooth surfaces for the final nanowires shown in Figures 1 and S4. However, the kinks still remained, giving the nanowires a “wavy” appearance.

The observations by TEM imaging indicate that particle attachment as assisted by CTAB templates<sup>11</sup> played a role in the formation of the wavy nanowires. This mechanism was supported by the fact that the diameter of the intermediate, necklace-like Au nanostructures, was essentially the same as that of the large Au nanoparticles formed in the early stage of a synthesis. In this case, the attachment of two Au nanoparticles with the same orientation was most favored in terms of energy reduction.<sup>8c</sup> In addition, twin boundaries were also observed in the resultant Au nanowires, presumably due to the participation of Au nanoparticles with different orientations as well as the involvement of twinned nanoparticles in the attachment (Figure S5). Besides particle attachment, cold welding<sup>12</sup> might also be involved in the formation of the Au wavy nanowires. This could occur wherever two adjacent Au nanostructures were overlapped or in physical contact with each other. The spontaneous welding of two adjacent Au nanostructures could be attributed to surface diffusion of the Au atoms. Thanks to the relatively low energy barrier, the Au atoms were able to diffuse rapidly on the surface of a Au nanostructure even at room temperature, leading to

successful welding. The slight reduction in diameter observed for the resultant wavy nanowires with respect to the intermediate nanostructures could also be attributed to surface diffusion and an elongation process. Alternatively, it can be attributed to additional deposition of the newly reduced Au atoms. When the freshly formed Au atoms collided with the surface of a Au nanostructure, the resultant Au adatoms could serve as “glues” to promote welding. It should be pointed out that besides the “head to head” geometry, the “head to side” and “side to side” configurations could also occur during the synthesis (Figure S6), resulting in the formation of some Au dendrites and nanosheets in the final products (Figure S7). Such Au nanostructures typically existed in small quantities and would precipitate to the bottom during a synthesis due to their large masses.

Since Au has a much higher density than water does, it is quite surprising and interesting that the Au wavy nanowires spontaneously accumulated at the air/water interface during a synthesis, which distinctly differs from the fabrication of straight, ultrathin Au nanowires in a bulk solution in the presence of small surfactant molecules.<sup>7c,8c,e,11b</sup> We conducted a control experiment by following the standard protocol except that the new reaction system contained an oil/water interface instead of an air/water interface. The resultant nanowires were also enriched at the oil/water interface (Figure S8), implying that the accumulation of Au nanowires at the air/water interface was likely caused by changes to their surface properties, rather than by physical trapping. In this case, the formation of a hydrophobic surface seems to be responsible for the separation of the wavy nanowires from the bulk of an aqueous solution. As reported in literature, CTAB molecules typically adsorb on the surface of a Au nanostructure in the form of a bilayer to form a hydrophilic outer layer so the nanostructure can be well dispersed in the bulk of an aqueous solution.<sup>13</sup> With regard to the formation of a hydrophobic surface, we suspect that it was associated with a structural change from a bilayer to a monolayer for the CTAB molecules adsorbed on the Au nanowires. To verify our hypothesis, we analyzed the nanowires by X-ray photoelectron spectroscopy (XPS) with the conventional Au nanorods (see Figure S9 for TEM image) serving as a reference. As shown by the survey spectra in Figure 3A, there were peaks for Br 3d, Au 4f,

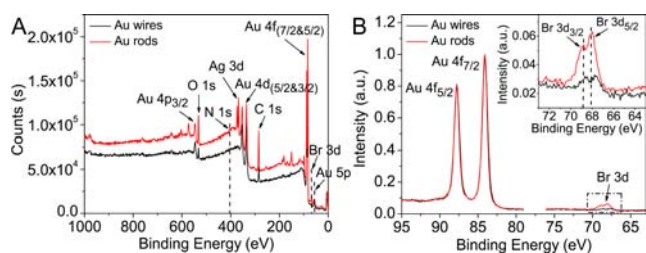


**Figure 3.** (A) XPS survey spectra of the Au wavy nanowires and Au nanorods showing the peaks for Au 4f, Br 3d, C 1s, N 1s, and O 1s. (B) Normalized XPS spectra of the Au 4f and Br 3d region collected with a resolution of 0.1 eV. Inset is the corresponding Br 3d region.

C 1s, and N 1s, indicating the existence of CTAB molecules on the surfaces of both types of Au nanostructures. In addition, the XPS spectrum of the Au nanorods contained the Ag 3d peaks due to the involvement of Ag<sup>+</sup> ions in the synthesis. Figure 3B shows high-resolution XPS spectra of the Au 4f and Br 3d peaks. After normalizing the intensity to the Au 4f<sub>7/2</sub> peak, we found that the intensity of the Br 3d peaks of the Au wavy nanowires was only about half of the corresponding intensity for the Au nanorods

(see Figure 3B inset). In addition, relative to bulk CTAB (see Figure S10), the Br 3d peaks blue-shifted after binding to the Au surface. Taking the peak of Br 3d<sub>5/2</sub> as an example, it was at 68.7 eV for the bulk CTAB, while it was shifted to 67.7 and 68.1 eV for the Au wavy nanowires and nanorods, respectively. The larger shifts of both the Br 3d peaks for the Au wavy nanowires imply that the Au–Br interaction was stronger on the surface of Au wavy nanowires than the nanorods. Considering that the CTAB molecules adsorbed on the surface of a Au nanorod in the form of a bilayer,<sup>13</sup> it is not unreasonable to conclude that the CTAB molecules only assembled into a monolayer or even submonolayer on the surface of a Au wavy nanowire.

We further used thermogravimetric analysis (TGA) to quantitatively measure the amount of CTAB molecules adsorbed on the surface of the Au wavy nanowires. As shown in Figure S11, the 0.82% weight loss between 100 and 750 °C could be ascribed to the decomposition and desorption of the CTAB molecules from the Au surface. Based on the area (0.64 nm<sup>2</sup>) occupied by the headgroup of an individual CTAB molecule,<sup>13c</sup> the average diameter (15 nm), and length (75 μm) of the Au wavy nanowires, the weight percentage of a perfect monolayer of CTAB molecules adsorbed on the surface of a Au nanowire was estimated to be 1.29% (see SI for details). This result further confirmed that the CTAB molecules only assembled into a monolayer or even a submonolayer on the surface of a Au wavy nanowire, generating a hydrophobic surface. As a result, the Au wavy nanowires spontaneously separated from the bulk of the aqueous solution in the late stage of a synthesis.

Figure 4 schematically illustrates how the Au wavy nanowires were formed due to changes to their surface properties. Since the concentration of CTAB molecules in the reaction system was much higher than the critical micelle concentration, the CTAB molecules should assemble into micelles in the solution, with the hydrophilic heads oriented toward water.<sup>14</sup> The CTAB bilayer adsorbed on the Au surface could also be considered as an “admicelle”,<sup>15</sup> which was composed of a monolayer of inner CTAB inverse micelle binding to the Au surface, covered by another monolayer of outer CTAB micelle to help stabilize the Au nanostructures in an aqueous solution. At the early stage of a synthesis, the relatively small Au nanoparticles and their aggregates were capped by a bilayer of CTAB admicelles because there were sufficient CTAB molecules in the solution (Figure 4A). Thanks to the flexibility of a micelle structure, the CTAB bilayer could easily merge together in an effort to accommodate the morphological change during particle attachment and welding when two Au nanoparticles came into close proximity

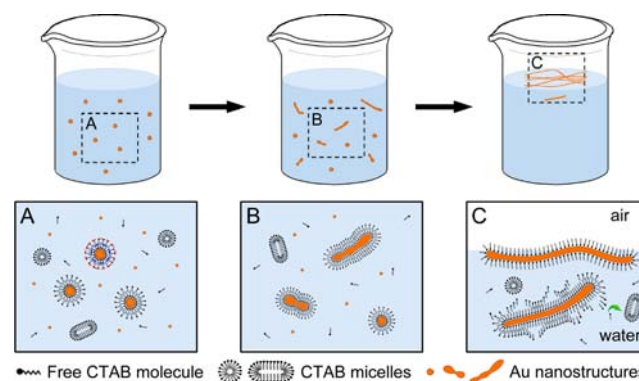


**Figure 4.** The surface of a Au nanostructure changes from a hydrophilic bilayer to a hydrophobic monolayer during the synthesis.



(Figure 4B). During this process, the CTAB admicelles might even serve as templates to assist the formation of 1D Au nanostructures. Although the small admicelle had a larger specific surface area (or surface to volume ratio) than the wavy nanowire, the nanowire had a much larger total surface area. When the total surface area of the elongated Au nanostructure exceeded the critical size allowed for the CTAB admicelles,<sup>14</sup> it would be difficult for the CTAB bilayer admicelle to maintain its structure and still cover the entire surface of a Au nanostructure due to a relatively weak binding between the outer and the inner layers of CTAB molecules. As a result, the outer layer of CTAB molecules would break into smaller micelles or even free CTAB molecules and thus desorb from the surface of the Au nanostructure (Figure 4C). As driven by the hydrophobic surface, the Au wavy nanowires or similar structures capped by CTAB monolayers (in the form of inverse micelles) started to separate from the bulk of the aqueous solution and migrate to the air/water interface. To validate the proposed mechanism, we also conducted a similar synthesis by replacing the CTAB in a standard procedure with CTAC at the same concentration. In this case, although the products were irregular nanoparticles rather than wavy nanowires, the nanoparticles also spontaneously separated from the bulk phase and floated at the air/water interface (Figure S12).

In summary, we demonstrate a simple approach to Au wavy nanowires with extremely high aspect ratios that spontaneously moved to the air/water interface during the synthesis. By analyzing the samples obtained at different stages of a synthesis, we found that both particle attachment and cold welding were involved in the formation of such nanowires. We further analyzed the Au nanowires by XPS and TGA, and the results indicate that the CTAB molecules changed their structure from a bilayer to a monolayer, converting the initially hydrophilic surface into a hydrophobic surface. As a result, the Au nanowires spontaneously migrated to the air/water interface. This approach is potentially extendable to many other systems involving the use of small surfactants as the capping agents.

## ■ ASSOCIATED CONTENT

### Supporting Information

Experimental details and characterization data. This material is available free of charge via the Internet at <http://pubs.acs.org>.

## ■ AUTHOR INFORMATION

### Corresponding Author

younan.xia@bme.gatech.edu

### Notes

The authors declare no competing financial interest.

## ■ ACKNOWLEDGMENTS

This work was supported partly by the NSF (DMR-1215034) and startup funds from Georgia Institute of Technology. C.Z., visiting from Southeast University, was partially supported by a fellowship from the China Scholarship Council. Some work was performed at the IEN at Georgia Tech and its cleanroom facilities, a member of NNIN sponsored by the NSF.

## ■ REFERENCES

- (1) (a) Lee, S. B.; Martin, C. R. *J. Am. Chem. Soc.* **2002**, *124*, 11850. (b) Tang, Z.; Kotov, N. A. *Adv. Mater.* **2005**, *17*, 951. (c) Burda, C.; Chen, X.; Narayanan, R.; El-Sayed, M. A. *Chem. Rev.* **2005**, *105*, 1025. (d) Murphy, C. J.; Gole, A. M.; Hunyadi, S. E.; Orendorff, C. J. *Inorg. Chem.* **2006**, *45*, 7544. (e) Hurst, S. J.; Payne, E. K.; Qin, L.; Mirkin, C. A. *Angew. Chem., Int. Ed.* **2006**, *45*, 2672. (f) Chen, J.; Wiley, B. J.; Xia, Y.

*Langmuir* **2007**, *23*, 4120. (g) Grzelczak, M.; Pe'rez-Juste, J.; Mulvaney, P.; Liz-Marza'n, L. M. *Chem. Soc. Rev.* **2008**, *37*, 1783. (h) Huang, X.; Neretina, S.; El-Sayed, M. A. *Adv. Mater.* **2009**, *21*, 4880.

- (2) (a) Rodrigues, V.; Fuhrer, T.; Ugarte, D. *Phys. Rev. Lett.* **2000**, *85*, 4124. (b) Wang, Q.-Q.; Han, J.-B.; Guo, D.-L.; Xiao, S.; Han, Y.-B.; Gong, H.-M.; Zou, X.-W. *Nano Lett.* **2007**, *7*, 723. (c) Zhang, C.; Barnett, R. N.; Landman, U. *Phys. Rev. Lett.* **2008**, *100*, 046801. (d) Zhang, X.; Liu, H.; Tian, J.; Song, Y.; Wang, L. *Nano Lett.* **2008**, *8*, 2653. (e) Yoo, S. M.; Kang, T.; Kim, B.; Lee, S. Y. *Chem.—Eur. J.* **2011**, *17*, 8657. (f) Oo, T. Z.; Mathews, N.; Xing, G.; Wu, B.; Xing, B.; Wong, L. H.; Sum, T. C.; Mhaisalkar, S. G. *J. Phys. Chem. C* **2012**, *116*, 6453.

- (3) (a) Hutchinson, T. O.; Liu, Y.-P.; Kiely, C.; Kiely, C. J.; Brust, M. *Adv. Mater.* **2001**, *13*, 1800. (b) Cross, C. E.; Hemminger, J. C.; Penner, R. M. *Langmuir* **2007**, *23*, 10372.

- (4) (a) Ramanath, G.; D'Arcy-Gall, J.; Maddanimath, T.; Ellis, A. V.; Ganesan, P. G.; Goswami, R.; Kumar, A.; Vijayamohan, K. *Langmuir* **2004**, *20*, 5583. (b) Xiong, S.; Molecke, R.; Bosch, M.; Schunk, P. R.; Brinker, C. J. *J. Am. Chem. Soc.* **2011**, *133*, 11410. (c) Huang, X.; Li, S.; Wu, S.; Huang, Y.; Boey, F.; Gan, C. L.; Zhang, H. *Adv. Mater.* **2012**, *24*, 979.

- (5) (a) Kim, F.; Sohn, K.; Wu, J.; Huang, J. *J. Am. Chem. Soc.* **2008**, *130*, 14442. (b) Critchley, K.; Khanal, B. P.; Go'rzny, M. L.; Vigderman, L.; Evans, S. D.; Zubarev, E. R.; Kotov, N. A. *Adv. Mater.* **2010**, *22*, 2338.

- (6) (a) Liu, X.; Wu, N.; Wunsch, B. H.; Barsotti, R. J., Jr.; Stellacci, F. *Small* **2006**, *2*, 1046. (b) Zhao, N.; Wei, Y.; Sun, N.; Chen, Q.; Bai, J.; Zhou, L.; Qin, Y.; Li, M.; Qi, L. *Langmuir* **2008**, *24*, 991.

- (7) (a) Wang, J. G.; Tian, M. L.; Mallouk, T. E.; Chan, M. H. W. *J. Phys. Chem. B* **2004**, *108*, 841. (b) Bai, H.; Xu, K.; Xu, Y.; Matsui, H. *Angew. Chem., Int. Ed.* **2007**, *46*, 3319. (c) Lu, X.; Yavuz, M. S.; Tuan, H.-Y.; Korgel, B. A.; Xia, Y. *J. Am. Chem. Soc.* **2008**, *130*, 8900. (d) Huo, Z.; Tsung, C.-K.; Huang, W.; Zhang, X.; Yang, P. *Nano Lett.* **2008**, *8*, 2041. (e) Ding, M.; Sorescu, D. C.; Kotchey, G. P.; Star, A. *J. Am. Chem. Soc.* **2012**, *134*, 3472.

- (8) (a) Jana, N. R.; Gearheart, L.; Murphy, C. J. *J. Phys. Chem. B* **2001**, *105*, 4065. (b) Nikoobakht, B.; El-Sayed, M. A. *Langmuir* **2001**, *17*, 6368. (c) Halder, A.; Ravishankar, N. *Adv. Mater.* **2007**, *19*, 1854. (d) Li, Z.; Tao, J.; Lu, X. M.; Zhu, Y.; Xia, Y. *Nano Lett.* **2008**, *8*, 3052. (e) Wang, C.; Hu, Y.; Lieber, C. M.; Sun, S. *J. Am. Chem. Soc.* **2008**, *130*, 8902. (f) Xu, Z.; Shen, C.; Sun, S.; Gao, H.-J. *J. Phys. Chem. C* **2009**, *113*, 15196.

- (9) (a) Halder, A.; Ravishankar, N. *J. Phys. Chem. B* **2006**, *110*, 6595. (b) Li, C.; Shuford, K. L.; Park, Q.-H.; Cai, W.; Li, Y.; Lee, E. J.; Cho, S. O. *Angew. Chem., Int. Ed.* **2007**, *46*, 3264. (c) Zeng, J.; Ma, Y.; Jeong, U.; Xia, Y. *J. Mater. Chem.* **2010**, *20*, 2290.

- (10) Zhou, J.; Zeng, J.; Grant, J.; Wu, H.; Xia, Y. *Small* **2011**, *7*, 3308.

- (11) (a) Yu, J. H.; Joo, J.; Park, H. M.; Baik, S.-I.; Kim, Y. W.; Kim, S. C.; Hyeon, T. *J. Am. Chem. Soc.* **2005**, *127*, 5662. (b) Feng, H.; Yang, Y.; You, Y.; Li, G.; Guo, J.; Yu, T.; Shen, Z.; Wu, T.; Xing, B. *Chem. Commun.* **2009**, *15*, 1984. (c) Kundu, P.; Halder, A.; Viswanath, B.; Kundu, D.; Ramanath, G.; Ravishankar, N. *J. Am. Chem. Soc.* **2010**, *132*, 20. (d) Wang, L.; Zhu, Y.; Xu, L.; Chen, W.; Kuang, H.; Liu, L.; Agarwal, A.; Xu, C.; Kotov, N. A. *Angew. Chem., Int. Ed.* **2010**, *49*, 5472.

- (12) (a) Ferguson, G. S.; Chaudhury, M. K.; Sigal, G. B.; Whitesides, G. M. *Science* **1991**, *253*, 776. (b) Lu, Y.; Huang, J. Y.; Wang, C.; Sun, S.; Lou, J. *Nat. Nanotechnol.* **2010**, *5*, 218. (c) Bi, Y.; Ye, J. *Chem. Commun.* **2010**, *46*, 6912. (d) Ishida, T.; Kakushima, K.; Fujita, H. *J. Appl. Phys.* **2011**, *110*, 104310. (e) Pereira, Z. S.; da Silva, E. Z. *J. Phys. Chem. C* **2011**, *115*, 22870.

- (13) (a) Jana, N. R.; Gearheart, L. A.; Obare, S. O.; Johnson, C. J.; Edler, K. J.; Mann, S.; Murphy, C. J. *J. Mater. Chem.* **2002**, *12*, 2909. (b) Nikoobakht, B.; El-Sayed, M. A. *Chem. Mater.* **2003**, *15*, 1957. (c) Sau, T. K.; Murphy, C. J. *Langmuir* **2004**, *20*, 6414.

- (14) (a) Imae, T.; Kamiya, R.; Ikeda, S. *J. Colloid Interface Sci.* **1985**, *108*, 215. (b) Pileni, M.-P. *Nat. Mater.* **2003**, *2*, 145.

- (15) (a) Harwell, J. H.; Hoskins, J. C.; Schechter, R. S.; Wade, W. H. *Langmuir* **1985**, *1*, 251. (b) Alkilany, M. A.; Frey, R. L.; Ferry, J. L.; Murphy, C. J. *Langmuir* **2008**, *24*, 10235.